Automotive Experiences
Vol. 6 No. 3 (2023) pp. 669-686
p-ISSN: 2615-6202 e-ISSN: 2615-6636

Research Paper

Tribology Properties on 5W-30 Synthetic Oil with Surfactant and Nanomaterial Oxide Addition

Poppy Puspitasari[1,2], **Avita Ayu Permanasari**[1,2], **Ayu Warestu**[1], **Gilang Putra Pratama Arifiansyah**[1], **Diki Dwi Pramono**[1], **Timotius Pasang**[3]

[1]Department of Mechanical and Industrial Engineering, Universitas Negeri Malang, 65145, Indonesia
[2]Centre of Advanced Material and Renewable Energy, Universitas Negeri Malang, 65145, Indonesia
[3]Department of Manufacturing and Mechanical Engineering and Technology, Oregon Institute of Technology, 97601, United States

poppy@um.ac.id

https://doi.org/10.31603/ae.10115

Check for updates

Published by Automotive Laboratory of Universitas Muhammadiyah Magelang collaboration with Association of Indonesian Vocational Educators (AIVE)

Article Info
Submitted: 30/08/2023
Revised: 08/11/2023
Accepted: 27/12/2023
Online first: 28/12/2023

Abstract

This study analyzes the tribological properties of 5W-30 synthetic oil with the addition of surfactants and oxide nanomaterials. This research used SAE 5W-30 lubricant base material with the addition of Aluminum Oxide (Al_2O_3), Titanium Dioxide (TiO_2), and Hybrid Aluminum Oxide (Al_2O_3) - Titanium Dioxide (TiO_2) nanomaterials. The nano lubricants were synthesized using a two-step method by adding nanomaterials by 0.05% volume fraction, followed by 50 ml of 5W-30 synthetic oil and polyvinylpyrrolidone (PVP) surfactant by 0.1%. Then, it was stirred using a magnetic stirrer for 20 minutes, followed by an ultrasonic homogenizer process for 30 minutes. Further, the nanolubricant was tested to identify its thermophysical properties, including density, dynamic viscosity, and sedimentation. It also underwent tribological testing, including wear, coefficient of friction, and surface roughness. Further, the nanomaterial was characterized using SEM, XRD, and FTIR. The morphological analysis using SEM suggested an irregular shape of the Al_2O_3 nanomaterial surface, while TiO_2 has a spherical shape. Besides, phase identification with XRD testing showed corundum and anatase phases. Functional group analysis through the FTIR showed the presence of Ti-O and Al-O. The highest density and viscosity results without surfactants were obtained in hybrid nanolubricant 779 kg/mm^3 and 0.0579 Pa.s, while the use of surfactants resulted in 788.89 kg/mm^3 of density and 0.0695 Pa.s viscosity. Tribological gray cast iron FC25 results in the best COF value observed in SAE 5W-30 + PVP-TiO_2 lubrication (0.093). The lowest wear mass without surfactant was obtained in the Al_2O_3-TiO_2 nanolubricant hybrid (0.02 grams), the lowest surface roughness in a mixture of PVP and TiO_2 surfactants was 0.743 μm. Meanwhile, the surface morphology of gray cast iron FC25 with hybrid nanolubricant SAE 5W-30 (Al_2O_3-TiO_2) and Nanolubricant SAE 5W-30+ (PVP-TiO_2) produced the smoothest surface.

Keywords: Oil 5W-30; Al_2O_3, TiO_2; Surfactan; Nanolubricant; Tribology

1. Introduction

Population growth in Indonesia which is increasing every year has an impact on the need for adequate transportation to support human activities. To meet human needs related to transportation, the automotive industry has also increased production by 10% annually since 2018 [1]. Along with the increasing population of vehicles, it must be directly proportional to the production of spare parts and lubricants that can support the maintenance of automotive vehicles, more specifically motorcycles. General lubricants are a necessity in the automotive world because they play an important role in reducing circulation between components to support engine performance in maximum condition [2].

Lubricants in motorized vehicles also function as vibration dampers, coolers, and transport of dirt found in internal combustion engines [3]. Selection of the quality of the lubricant according to the engine specifications can extend the service life of the vehicle and can improve the work performance and durability of the motorcycle engine. Using the wrong lubricant will cause a decrease in engine performance and component wear and tear which can lead to severe damage [4]. To reduce losses that occur in motorcycle engine components due to wear and tear, this can be done by considering the selection of the type of lubricant according to the required specifications.

Lubricants have a viscosity at high temperatures or low temperatures when the engine is operated, so lubricants have their own grade (degree) regulated by the Society of Automotive Engineers (SAE). The SAE 5W-30 number on the lubricant packaging means a viscosity of 5 at cold temperatures (winter), and a viscosity of 30 at 100 degrees Celsius [5]. Nanoparticles have been suggested as a lubricant additive to improve thermophysical performance. The addition of nanomaterials to base fluids changes their thermophysical features such as density, viscosity and thermal conductivity. The dimensions and shape of the nanomaterial, the concentration of the nanomaterial, the viscosity of the base fluid, and the surfactants used for the formulation are the main parameters that affect the performance of the lubricant [6].

The addition of oxide nanomaterials, such as Aluminum Oxide (Al_2O_3) and Titanium dioxide (TiO_2), on basic lubricant reduces friction and wear since Al_2O_3 has excellent heat transfer nature, while TiO_2 can quickly spread, resulting in more excellent surface quality [7]. Thus, the addition of polyvinylpyrrolidone (PVP) surfactant inhibits agglomeration on nanolubricant, enhances the efficiency, as well as decreases friction and wear on gray cast iron FC25 material [8].

Based on the description above, it is hoped that this research can be a solution in overcoming the problem of friction loss and wear caused by friction between the cylinder block and piston ring in vehicle engines. Apart from that, it can be a way to save fuel and extend engine life by paying attention to the type of lubrication used. This research focuses on studying tribological properties by synthesizing nanolubricants added with Al_2O_3 and TiO_2 nanomaterials and 5W-30 synthetic oil as well as adding polyvinylpyrrolidone (PVP) as a surfactant additive to gray cast iron FC25 specimens.

2. Method

2.1. Additive Materials

In this study, Aluminum Oxide from SIGMA ALDRICH dengan with 99.5% was used, with white color and powder shape at an average size ≤ 10 μm. Meanwhile, Titanium Dioxide nanoparticle is formed from titanium oxide. Titanium oxide (TiO_2) is a widely accessible dielectric nanomaterial with high thermal conductivity properties. Besides, Titanium Dioxide (TiO_2) can precipitate and improve the properties of base oil, as well as carrying sufficiently low concentration for conquering friction [9]. In this study, Titanium Dioxide brand SIGMA ALDRICH with 99.7% purity, white color, and powder form (average particle size of ≤ 25 nm) was used.

Surfactant is a critical component in the preparation of nanolubricant. The addition of surfactant enhanced the nanoparticle's dispersion stability [10]. It had hydrophobic tails and hydrophilic heads. The polyvinylpyrrolidone (PVP) was used as the surfactant in this study. It is a commercial, industrial polymer with a low cost that has been commonly utilized in numerous fields, such as lithium batteries, water electrolysis, anti-bacterial agents, food additives, and surfactants [11]. Polyvinylpyrrolidone (PVP) is also referred to as a nonionic polymer containing robust hydrophilic molecules and can adhere easily to materials in solution [12]. PVP has also been reported to lower the repulsive force between hydrophobic chains in materials containing two atoms in one molecule [13]. The structure of polyvinylpyrrolidone (PVP) is presented in **Figure 1**.

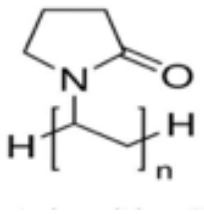

Figure 1. Structure of polyvinylpyrrolidone (PVP)

2.2. Additive Materials Characterization

Material characterization was carried out to identify the properties of the material. This research used three types of characterization, including SEM (Scanning Electron Microscopy), to identify the surface morphology of nanoparticles [14], XRD (Xray-Diffraction), and FTIR (Fourier Transform Infrared). The XRD was used to determine the crystalline phase structure of nanoparticles by investigating the the material [15]. Lastly, the FTIR (Fourier Transform Infrared) was performed to find the functional group using infrared [16].

2.3. Nanolubricant Preparation

SAE 5W-30 nanolubricant was used as the base oil. In this study, seven samples with 0.05% fraction volume were prepared, consisting samples 5W-30 base oil, Al_2O_3 nanolubricant + SAE 5W-30, TiO_2 nanolubricant + SAE 5W-30, hybrid nanolubricant Al_2O_3 - TiO_2 +SAE 5W-30, as well as the samples with the same volume fraction added with polyvinylpyrrolidone (PVP) surfactant. After the samples had been prepared, the lubricant and nanoparticle were stirred using a magnetic stirrer at 1250 rpm speed and room temperature for 20 minutes. Then, we conducted homogenization using an ultrasonic homogenizer for 30 minutes to produce a nanolubricant with excellent stability. The prepared nanolubricant with and without Polyvinylpyrrolidone (PVP) surfactant are illustrated in **Figure 2a** and **Figure 2b**.

2.4. Nanolubricant Characterization

2.4.1. Analisys of Thermophysical Properties

Thermophysical properties determine the performance, pressure drop, heat transfer coefficient, and thermal efficiency of a system [17]. The thermophysical properties parameters for nanolubricant include viscosity and density. Viscosity indicates the amount of force needed to move an object in a fluid. Besides, it can serve as an indicator of fluid viscosity, reflecting the level of friction within the fluid [18]. In this study, Viscometer type NDJ-8S was utilized, with rotor number 1 and different speeds of 6 rpm, 12 rpm, 30 rpm, and 60 rpm, as well as temperature ranging between 30 °C – 100 °C. Further, Eq. (1) was used to estimate the dynamic viscosity.

$$\upsilon = \frac{\mu}{\rho} \tag{1}$$

Where, υ = Kinematic viscosity (m^2/s); μ = Dynamic viscosity (kg/m.s); ρ =density (kg/m^3)

Density represents the mass per unit volume that is symbolized by (Rho) with the international unit of kg/m^3 and a British unit of slug/ft3 [19]. The density of fluid was calculated using Eq. (2).

$$\rho = \frac{m}{V} \tag{2}$$

Where, ρ = density (kg/m^3); m = masss of fluid (kg); V = Fluid volume (m^3).

2.4.2. Analysis of Tribology Properties

Tribology is the study of friction, wear, and lubrication [20]. In a more extensive range, tribology is defined as a reciprocal relationship between the surface of a solid and a moving object, as well as the reasons for its emergence. For the tribology analysis, we used the pin-on-disc tribometer. In specific, we used the pin on disc from Stainlees steel, named Ducom Instruments,

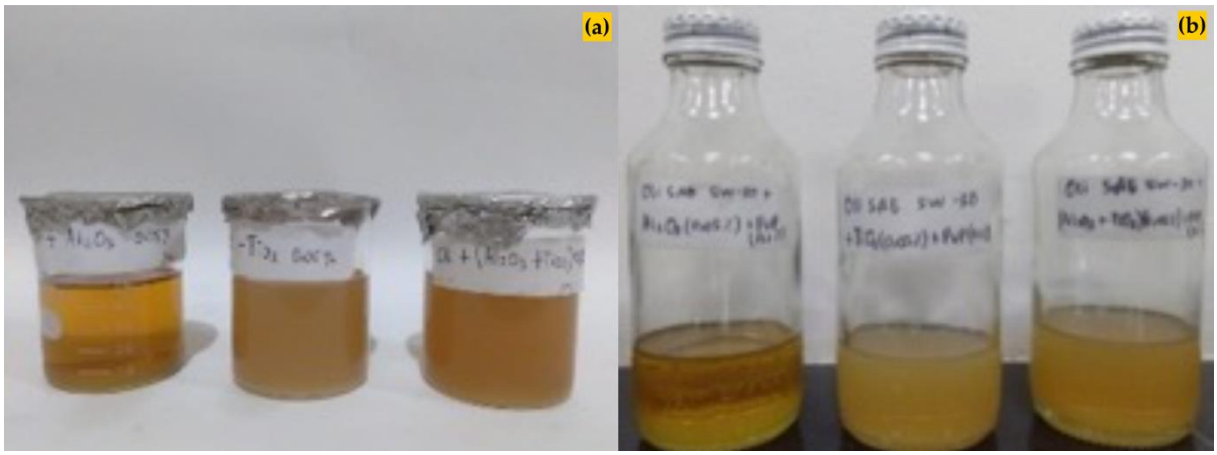

Figure 2. Prepared nanolubricant (a) without surfactant and (b) with polyvinylpyrrolidone (PVP) surfactant

with blue display, digital display type, 3-12 mm pin diameter and 165 x 8 mm disc diameter, and a load capacity of 5 - 200 N. Tribometer pin on the disc contains pins and discs that are commonly used to measure friction and wear. The schematic of the pin-on-disc test equipment is illustrated in **Figure 3a**, while the rotary movement of the pin-on-disc is shown in **Figure 3b**.

One of the applicable instruments for this analysis is the pin on the disc, where the disc rotates while the pin is motionless and pressed against the disc. This frictional loading will result in repeated contact between surfaces, which will eventually take some of the material on the surface of the pin on the disc [21]. Friction and wear have a close correlation with tribology testing as friction represents the interaction between two nudging surfaces with relatively constant movement, while wear is the gradual loss of material from two nudging surfaces due to contact [22]. The friction and wear were estimated using Eq. (3) and Eq. (4), respectively.

$$\mu = \frac{F}{P} \tag{3}$$

Where, μ = Friction coefficient; F : Measured frictional force; P : The normal load attached to the pin seat

$$\Delta V = \frac{m_0 - m_1}{\rho} \tag{4}$$

Where, ΔV = Wear volume of a material (m^3); m_0 = Mass of specimen before testing (kg); m_1 : Mass of specimen after testing (kg); ρ = Specimens density (kg/m^3)

2.4.3. *Analysis of Surface Roughness*

The roughness analysis was completed using Stylush Probe or Surfcom Touch instrument. The roughness test was conducted on the disc surface which directly touched the pin. This surface roughness test was conducted to measure and analyze the roughness of a material or surface [23]. For the Surfcom Touch, we used the ones with code no. 178-395, speed of 1 mm/s, cable length of 1 m and mass of 190 g. The surfcom touch instrument used in this study is illustrated in **Figure 4**.

3. Result and Discussion

3.1. *Scanning Electron Microscopy (SEM) Analysis on Aluminum Oxide (Al_2O_3) and Titanium Dioxide (TiO_2)*

Scanning Electron Microscopy (SEM) on Aluminum Oxide (Al_2O_3) and Titanium Dioxide (TiO_2) nanomaterials was performed to identify their morphology [24], [25]. This test was carried out using SEM brand FEI type *Inspect*-S50 purchased in Japan. The obtained SEM characterization on Aluminum Oxide and Titanium Dioxide nanoparticles is illustrated in **Figure 5a**. and **Figure 5b**.

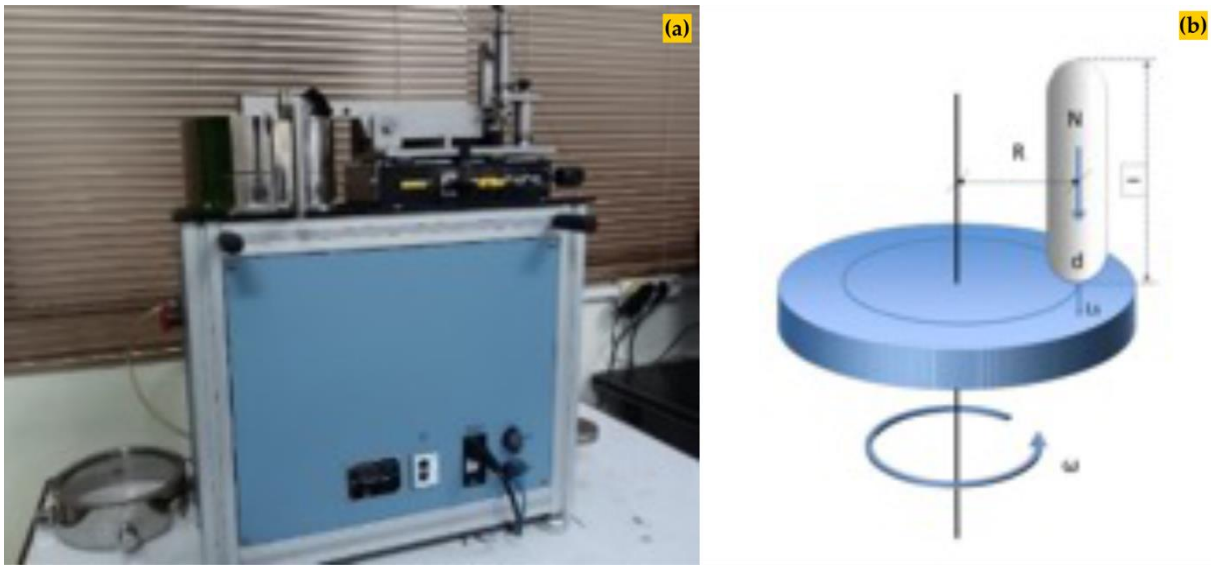

Figure 3. Tribology Test (a) Tribometer pin on disc (b) Rotating scheme of pin on disc tribometer (N= the force exerted on pin (N); R= distance between disc and pin (mm); D= ball/pin diameter (mm); W= rotation (rpm))

Figure 4. Surface roughness Instrument

The SEM analysis results on Aluminum Oxide and Titanium Dioxide at 1000x and 10000x magnification suggested the dominant presence of the Corundum phase (Al_2O_3) with trigonal crystal structure [26]. Meanwhile, the results of the microstructure test showed that the Aluminum Oxide nanomaterial has irregular grain shapes and nanoparticles that do not bind to each other. Further, the SEM analysis results on the titanium dioxide indicated its anatase phase with a tetragonal crystal structure, tendency to agglomerate, and spherical shape similar to a ball [27].

3.2. *X-Ray Diffraction (XRD) Analysis on Aluminum Oxide and Titanium Dioxide*

Section The X-Ray-Diffraction (XRD) test was carried out to identify the phase structure, crystallinity, and grain shape of Aluminum Oxide and Titanium Dioxide nanomaterials [28]. The analysis was performed explicitly on the diffraction peaks on the XRD graph. For the instrument, we adopted the Pananalytical brand typeE'xpert Pro equipped with SHP (Software High Score Plus) and PDF2. The results of the XRD test on Aluminum Oxide (Al_2O_3) and Titanium Dioxide (TiO_2) nanomaterials are presented in **Figure 6a** and **Figure 6b**.

As illustrated in **Figure 6a**, Al_2O_3 carries the highest peak intensity at 2teta angles of 25.47, 35.04, 37.67, 43.26, 52.45, 57.41, 66.42, 68.12, 76.80, which correspond to the miller index of (hkl) (012), (104), (110), (113), (204), (116), (214), (300), (119). The crystallite shape of *Aluminum Oxide* (Al_2O_3) was analyzed using MATCH *software*. The results showed a trigonal crystal shape, similar to the findings reported in a study [29] describing the trigonal crystal shape of (Al_2O_3). For calculating its crystallite size, the Scherrer formula (Eq. (2)) was conducted [30], [31].

$$D = \frac{K.\lambda}{\beta \cos\theta} \tag{4}$$

Where, D = Crystal size (nm); K = Form factor of the crystal (0.9); λ = X-ray wavelength (0.15406); β = Value of FWHM (Full Width at Half Maximum) (rad); θ : Diffraction angle (°)

The obtained crystallite size at 35.043 positions with an FWHM of 0.1224 was 68.0622 nm.

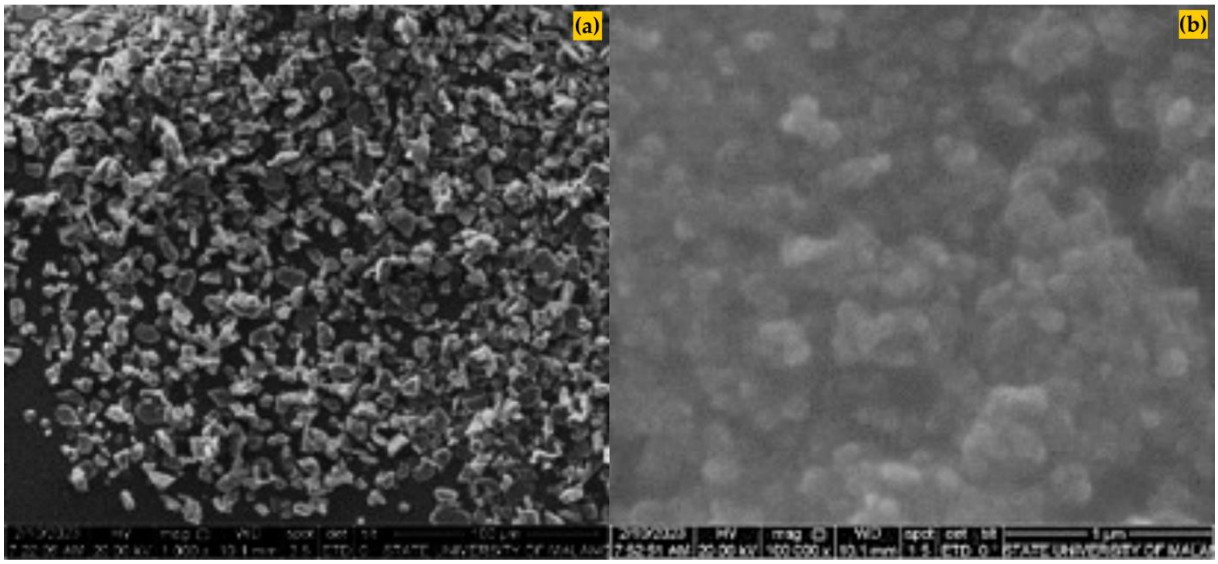

Figure 5. Results of SEM for (a) Aluminum oxide (Al_2O_3) at 1000x magnification and (b) Titanium dioxide (TiO) with 10000x magnification

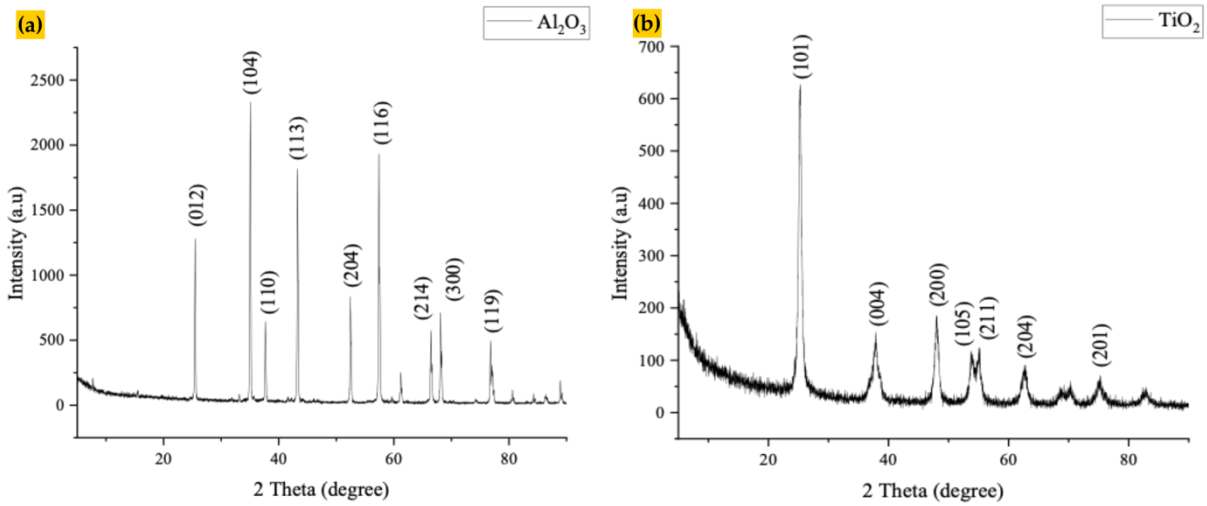

Figure 6. (a) XRD graph for Al_2O_3 nanomaterial; (b) XRD graph for TiO_2 nanomaterial

In addition, TiO_2 presents the highest peak intensity at 2teta angle: 25.35, 37.89, 47.95, 53.84, 55.12, 62.84, 75.13 with miller index value of (hkl) (101), (004), (200), (105), (211), (204), (201), as presented in **Figure 6b**. Besides, according to the Match software analysis results, TiO_2 has tetragonal crystal shape, linear to the results discovered in a study [32]. For its crystallite size, we performed calculations using the Scherrer equation, showing the 20.2806 nm crystallite size at 25.3464 position with FWHM of 0.4015.

3.3. *Fourier Transform Infrared (FTIR) Analysis on Aluminum Oxide and Titanium Dioxide*

The Fourier Transform Infrared (FTIR) test results indicate the content and functional groups of Al_2O_3 and TiO_2 nanomaterial. In this study, we used FTIR brand *Shimadzu* type *IRprestige* 21. The obtained data are in the form of graphics at around 4000-500 wavelength [33] **Figure 7a** and **Figure 7b**. depicts the FTIR spectrum for Al_2O_3 and TiO_2 around 4000-500 cm-1 wavelength.

Figure 7a shows that Al_2O_3 has O-H stretching bond at 3524 [34]. Besides, it also presents a C-H vibration bond [35], a symmetric bending Al-O-H vibration bond [36], [37] Al-O stretching bond [38] at 2309, 1058.99, and 400-800 peaks, respectively.

In addition, the Al_2O_3 has O – H stretching vibration at 3300 – 3500 [39], Ti-OH at 2300 and 1630 [40], along with bending Ti – OH and C – O stretching vibration at 1151-1106 and 1054-1041 [41], as well as Ti-O stretching bond and O-Ti-O at 895 and 500-70 peak, respectively [42].

3.4. *Sedimentation*

The nanolubricant stability test was carried out using the sedimentation method. The sedimentation method can only be observed visually by measuring the height of the mixture in 0, 4, 8, 12, 16, and 20 days [43]. The stability can be

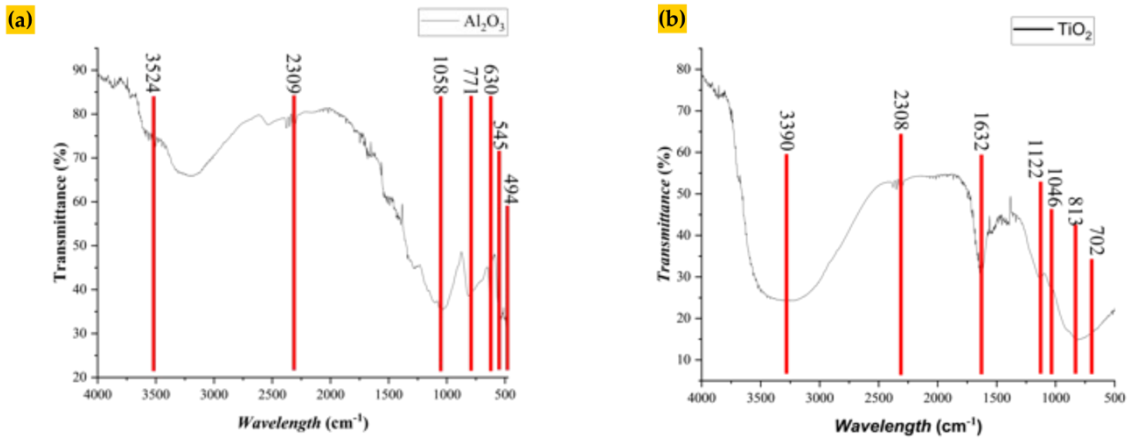

Figure 7. (a) FTIR spectrum for Al_2O_3 nanomaterial; (b) FTIR spectrum for TiO_2 nanomaterial

easily evaluated by taking a photo of the sedimentation of the sample in a beaker or clear bottle. Analysis using the sedimentation method is usually carried out immediately after the nanoparticle dispersion in the lubricant. Consequently, sedimentation time protects against wear and reduces friction [44].

3.5. *Density*

The density test involved measuring the weight of the fluid and then dividing it by its volume. The density test results for the nanolubricant added with and without PVP surfactant are shown in **Figure 8**.

Based on **Figure 8**, the highest density value for the 5W-30 hybrid nanolubricant is 779 kg/m^3, while the lowest density was observed on the 5W-30 base lubricant. The density value is influenced by several parameters, such as temperature, as well as the addition of chemical composition and additives [45]. In **Figure 8**, the density of lubricant added with surfactant is represented by the green stick. The highest density observed on TiO_2 added with PVP surfactant is 778,889 kg/m^3. As the nanoparticle density has been reported to affect the density of the prepared nanolubricant [46], [47], initially, the density of TiO_2 and Al_2O_3 is 4,23 and 3,7 g/cm^3, respectively. The addition of PVP surfactant in nanolubricant enhances its density, thus, the nanolubricant added with surfactant presents greater density [48].

3.6. *Viscosity*

The viscosity test was performed using the viscometer type NDJ-8S at 1 – 2000000 mPa.s. The obtained viscosity for the samples with and without PVP surfactant is presented in **Figure 9**, with the pink stick representing the results for samples with no surfactant addition, while the green stick shows the viscosity of samples with PVP surfactant. The results suggested that the basic lubricant with and without PVP surfactant presents 0.0442 Pa.s dynamic viscosity, while *nanolubricant* SAE 5W-30 + Al_2O_3, SAE 5W-30 + TiO_2, and *hybrid nanolubricant* + SAE 5W-30, have 0.0468, 0.0563, and 0.0579 Pa.s dynamic viscosity, respectively. This result is induced by the increase of internal shear stress at concentration with higher concentrations [49]. Further, the dynamic viscosity on the nanolubricant added with a surfactant is linear with their density since viscosity, as influenced by the nanoparticle's density. Meanwhile, the *hybrid* Al_2O_3-TiO_2 nanolubricant presents the features from both nanoparticles, thus, its dynamic viscosity lies between the two of them [50].

3.7. *Tribology*

3.7.1. *Surface Wear of Gray Cast Iron FC25 with Nanolubricant Variations*

Figure 10 shows average wear mass test results for gray cast iron FC 25 without and with surfactant. The bar in green represents the wear from no lubrication, with the highest wear of 0.082 grams. Meanwhile, the yellow bar shows the wear mass of SAE 5W-30 base oil which reaches 0.012 grams. The red bars show the wear mass from the nanolubricant added with PVP surfactant. The use of SAE 5W-30 + Al_2O_3 and SAE 5W-30 + TiO_2 nanolubricant results in 0.003 and 0.004 grams of

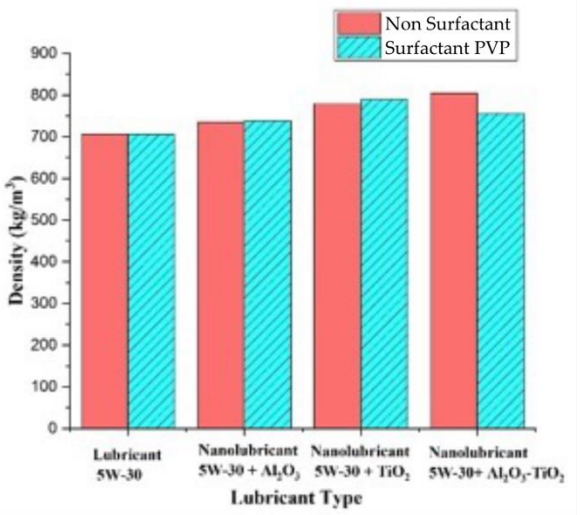

Figure 8. Density test results

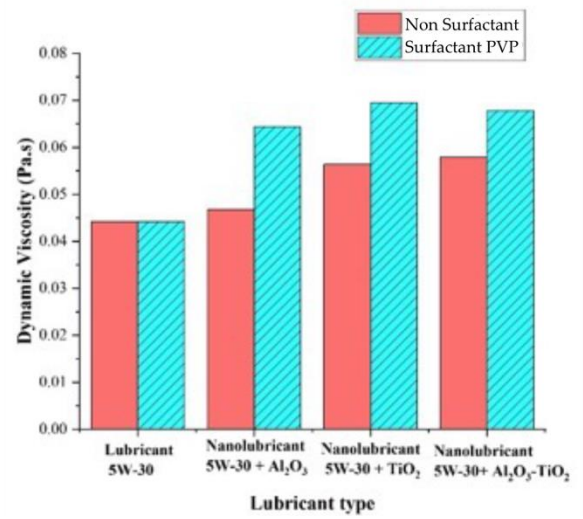

Figure 9. Viscocity of lubricant

wear mass. The lowest average wear for the samples with no surfactant was observed from the hybrid nanolubricant + SAE 5W-30 sample (0.002 gram). The lowest wear mass on the use of hybrid nanolubricant samples with no surfactant is caused by the addition of Al_2O_3 and TiO_2, which significantly lowers the wear mass, in comparison to the use of base oil or lubricant added with single oxide nanomaterial [51]. Additionally, the hybrid nanoparticle Al_2O_3 and TiO_2 is a modified additive that significantly reduces the friction coefficient, resulting in excellent anti-wear effects than the pure Al_2O_3 and TiO_2 [52]. Lastly, the blue chart in **Figure 10** shows the COF test results on samples added with surfactant. The addition of PVP surfactant on lubrication affects the wear of gray cast iron FC25, as illustrated in **Figure 10**. The lowest wear was observed on the samples added with TiO_2 due to the low friction coefficient of nanolubricant with PVP and TiO_2. The friction coefficient is directly proportional to the wear mass of gray cast iron FC25 [53]. The excellent stability of nanolubricant presents a positive contribution to the moving element due to the more extended period of nanoparticle agglomeration, which inhibits massive abrasive wear [54].

3.7.2. *Surface Friction Coefficient of Gray Cast Iron FC25 with Nanolubricant Variation*

Figure 11 presents the COF test results on gray cast iron FC25 with and without surfactant. The green bar represents the COF results with no lubrication of 0.727. This finding signifies that the higher COF is induced by the unlubricated gray cast iron surface, which results in wear and a greater amount of friction. The yellow bar in **Figure 11** shows the COF results for the SAE 5W-30 base oil lubrication, which reaches 0.108. The base oil on the friction surface decreases the severity of abrasion caused by the nanoparticle, which decelerates the COF value. The red bar represents the 0.154 COF results for the SAE 5W-30 + Al_2O_3 nanolubricant with no PVP. Meanwhile, the use of hybrid nanolubricant SAE 5W-30 results in a 0.143 value which does not significantly differ from the results of SAE 5W-30 nanolubricant. Further, the lowest COF result was found on the SAE 5W - 30 + TiO_2 nanolubricant (0.093), similar to the result reported in a study. That study further explained that the lowest COF value mainly occurs due to the reduction of the frictional torque due to the presence of nanoparticles which effectively transforms pure friction into scrolling friction. Besides, the spherical shape of Titanium Dioxide (TiO_2) nanoparticles can serve as the ball bearings that roll into the contact area, enabling the change of sliding friction into combination friction (sliding and rolling). Additionally, the lubrication also correlates with a tribo-pair system, which maintains the nanoparticle's stiffness and shape by establishing low and stable load among the friction surface, which results in better and

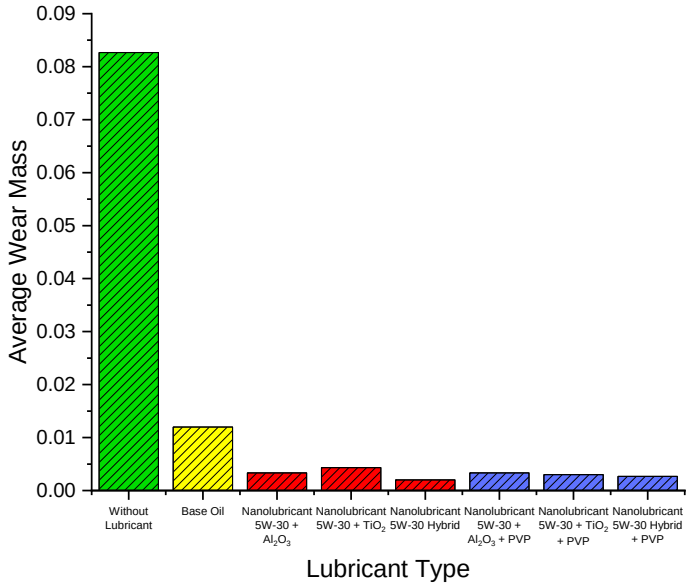

Figure 10. Wear test on gray cast iron FC25 with nanolubricant variation

smaller friction [55], [56]. The blue chart in **Figure 11** shows the COF results on the samples with surfactant addition. The highest friction coefficient test results on samples with PVP surfactant were identified on the Al_2O_3 + SAE 5W-30 samples (0.174), while the lowest was in TiO_2 + SAE 5W-30 (0.093). [57] described that the smaller nanoparticle size reduces friction. Meanwhile, the sphere shape nanoparticle presents a rolling effect between the surface, which enhances the wear endurance [58].

3.7.3. Surface Roughness of Gray Cast Iron FC25 with Lubricant Variations

Figure 12 illustrates the surface roughness test on gray cast iron FC25 with and without surfactant. The red bar represents the roughness in the Ra unit, while the blue bar shows the roughness in the Rq unit. The highest roughness of 1.67 μm Ra 2.12 μm Rq was found from the gray cast iron FC25 without lubrication, while for the gray cast iron FC25 with a base oil lubricant, we obtained 0.96 Ra and 1.17 μm Rq. Meanwhile, for the SAE 5W-30 + Al_2O_3 nanolubricant, .86 μm Ra and 096 μm Rq were obtained. The addition of Al_2O_3 into the basic lubricant enables the Al_2O_3 to bind the surface roughness and conductivity. Besides, the Al_2O_3 coating has been reported as an alternative for regulating surface roughness [59]. For the roughness test on gray cast iron, FC25 with lubrication using TiO_2 nanolubricant and PVP surfactant was identified as the lowest, with a

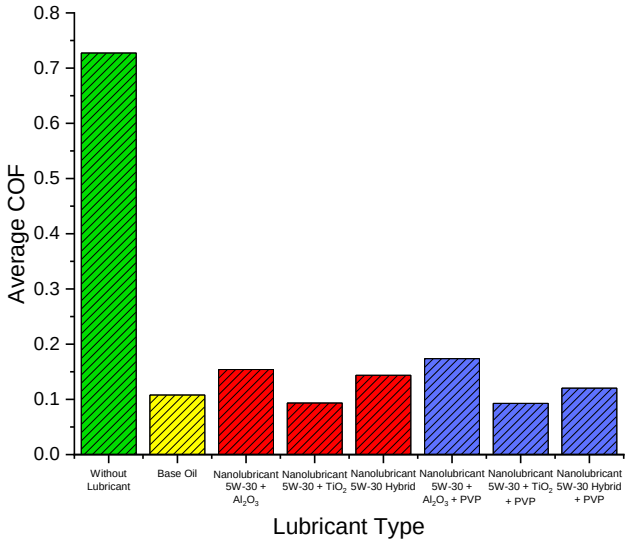

Figure 11. COF results on gray cast iron FC25 with nanolubricant variation

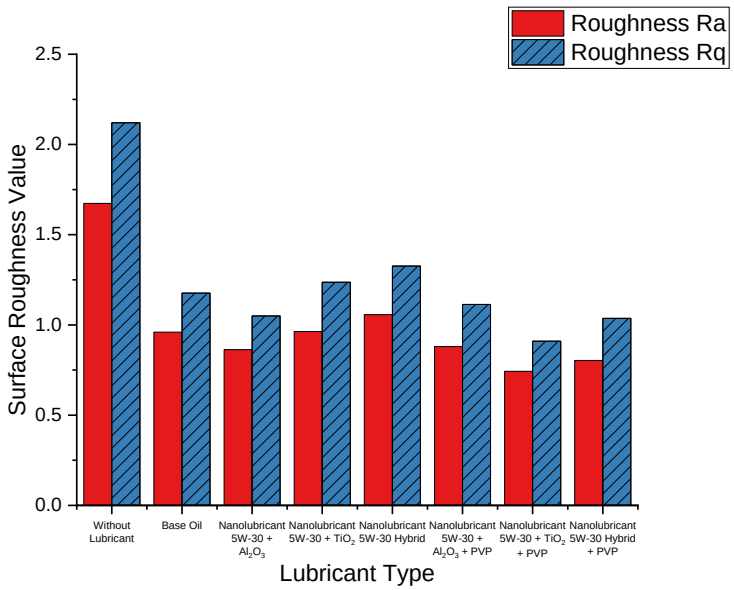

Figure 12. Surface roughness of gray cast iron FC25 with nanolubricant variation

roughness value of 0.743 μm. The results from Al2O3 nanolubricant + SAE 5W-30 and hybrid nanolubricant Al2O3 - TiO2 +SAE 5W-30 were 0.880 and 0.803 μm, respectively. The surface roughness is affected by the nanoparticle's abrasive nature [57], contact voltage, adhesion, and surface friction, which results in wear on the wear track and increases the surface roughness [60].

3.7.4. *Macroscopic Observations on Gray Cast Iron FC25*

The macroscopic observation was performed to analyze and identify the defects or damages on an object. Besides, it also facilitates the identification of cracks and corrosion. **Figure 13** shows the macro picture of the gray cast iron FC25.

Figure 13a–Figure 13h presents the result of macro photo observations on the surface of gray cast iron FC25 using 250x magnification. The macro photo observations in this study were divided into two, namely the observations on samples without surfactant (**Figure 13a–Figure 13e**) and the ones with surfactant (**Figure 13f–Figure 13h**). As presented in **Figure 13a**, the gray cast iron with FC25 without lubricant has dominant scratches on its surface with plastic deformation caused by high contact and debris [61]. **Figure 13b** shows the macro photo test of gray cast iron FC25 using base oil as a lubricant. It shows a dark area on its wear track which indicates the presence of an adhesive layer from debris or an interface layer established during the friction process. A study [62] uncovered that the SAE 5W-30 lubricant generates smaller friction due to its more excellent

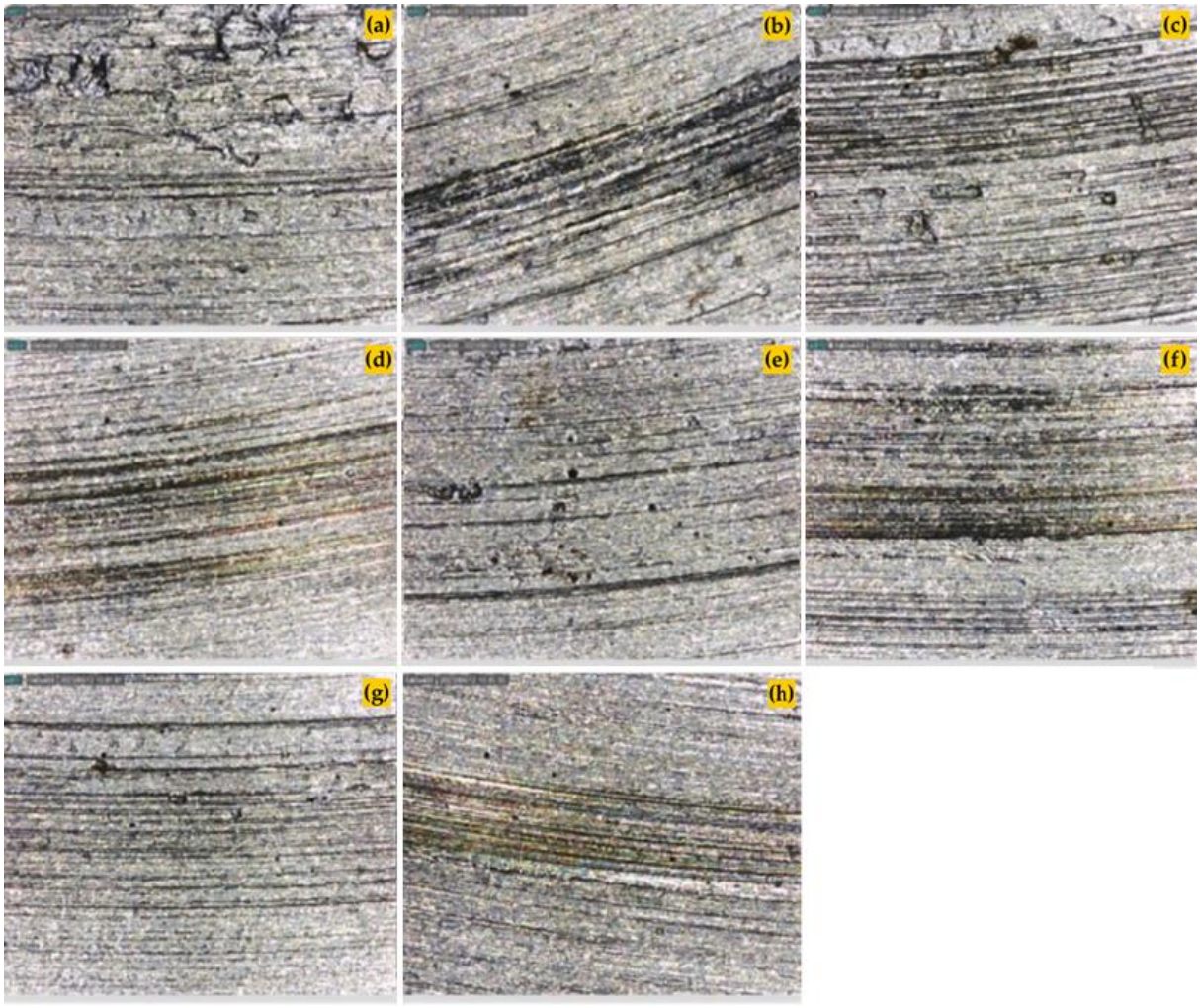

Figure 13. Macro Picture Observation (a) Without lubrication; (b) SAE 5W-30 base oil; (c) 5W-30 + (Al_2O_3) nanolubricant; (d) 5W-30 + (TiO_2) nanolubricant; (e) Hybrid 5W-30 + (Al_2O_3-TiO_2) nanolubricant; (f) 5W-30 + (Al_2O_3-PVP) nanolubricant; (g) 5W-30 + (TiO_2-PVP) nanolubricant; (h) Hybrid 5W-30 + (Al_2O_3-TiO_2-PVP) nanolubricant

properties. Further, the same study also describes the correlation between the friction diameter with the lubrication performance, in which the lower friction signifies greater lubrication performance. **Figure 13c** illustrates the test results for SAE 5W-30 + Al_2O_3 nanolubricant, while **Figure 13f** shows the results for SAE 5W-30 + PVP + Al_2O_3 nanolubricant. From those two figures, we observed more significant scratches from the results of samples with No. PVP. This scratch is caused by the addition of PVP, which activates the abrasive nature of Al_2O_3. Further, we also identified a clear dominating mechanical scratch on the wear surface, but it has lower dark areas in comparison to the SAE 5W-30 base oil sample. Linearly, [63] concluded that Al_2O_3 nanoparticle forms minor grooves on the contact surface induced by nanoparticle piracy effects. Meanwhile, **Figure 13d** shows the test results for SAE 5W-30 + TiO_2 nanolubricant, which indicates the specimen surface with a smother groove than the specimens coated with Al2O3 nanolubricant + SAE 5W-30, SAE 5W-30, and without lubricant. The addition of PVP surfactany on TiO_2 forms tribofilm layer on the gray cast iron FC25 surface. Therefore, the gray cast iron FC25 surface added with PVP + TiO_2 appears to be smooth, as presented in 13g. The addition of Titanium Dioxide lowers the friction and wear on the gray cast iron FC25 through the tribological reaction between the modified TiO_2, the nanoparticle's surface, and the gray cast iron FC25 surface during the sliding surface, along with the adsorption of decomposed particles [64]. Additionally, the photo macro analysis on the hybrid nanolubricant + SAE 5W-30 shows the role of Al_2O_3 + TiO_2 as the additive material tends to produce a smooth surface in comparison to the specimens with SAE 5W-30 + TiO_2 nanolubricant. The addition of PVP surfactant on hybrid Al_2O_3-TiO_2 generates a more significant size of scratch than from the specimens coated with nanolubricant with no surfactant because the addition of PVP induces abrasive Al_2O_3 on the surface of gray cast iron FC25. This finding is in accordance with the results of the wear mass test presented in **Figure 13g**. Besides, the addition of Al_2O_3 and TiO_2 hybrid nanoparticles on the basic oil (5W-30) fills the wear and curvature on the wear surface (a physical mechanism), aiding separation, reducing contact between metals, thereby providing a hydrodynamic effect that minimizes the coefficient of friction and making the surface smoother [65].

3.7.5. Morphology Observation on Wear Track of Gray Cast Iron FC25

Figure 14 and **Figure 15** present the SEM observation results on the surface morphology of gray cast iron FC25 using 30x and 100x magnification. The morphological observations in this study were divided into two, namely without polyvinylpyrrolidone surfactant (**Figure 14c-Figure 14e** and **Figure 15c-Figure 15e**) and with Polyvinylpyrrolidone surfactant (**Figure 14f-Figure 14h** and **Figure 15f-Figure 15h**). The result presented in **Figure 14a** and **Figure 15a** are the morphology of FC25 gray cast iron without the use of lub ricants. These two figures indicate greater roughness and wear on the specimen surface in comparison to the specimens with SAE-30 base oil lubricants and other variations of lubricants. On the specimens with no lubricant, we observed signs of extensive plastic deformation with deep grooves that appear on the wear track. This is in line with the statement xx. The emergence of plastic deformation is caused by thermal softening, which is formed due to repeated loading without base oil or lubricants. Besides, it also generates other signs, such as deep grooves and material removal, resulting in plastic deformation, abrasion, and delamination that determine the mechanisms causing the wear and tear. The porosity results after testing on samples without nanolubricant were 61,174%.

Furthermore, **Figure 14b** and **Figure 15b** shows the results of the wear track on the FC25 gray cast iron test with SAE 5W-30 base oil lubricant. The figures indicate the scratches that cause abrasion grooves in the traces where the pin hit the disc [66]. This surface wear signifies the decrease of collected tribofilm, causing friction between the contacts which results in a porosity of 41.2%, slightly lower than the specimens without lubricant. **Figure 14c** and **Figure 15c** illustrate the results of the wear track on FC25 gray cast iron coated with nanolubricant SAE 5W-30 and Al_2O_3, showing a fairly deep wear surface and plastic deformation, which causes wear on the surface. This is due to the continuously increasing number of indentations or grooves and levels of delamination resulting in erosion on the transfer

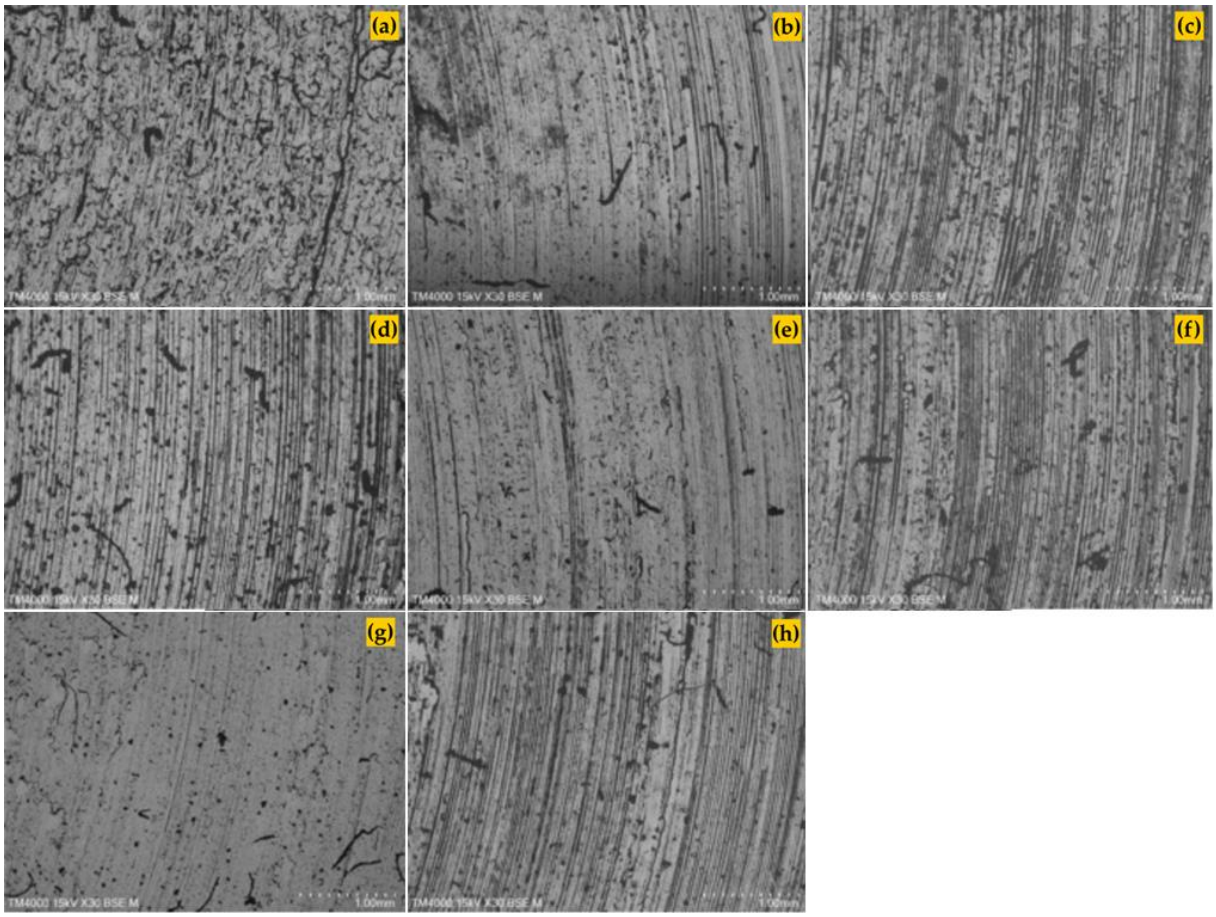

Figure 14. Morphology analysis on gray cast iron FC25 at 30x magnification (a) Without lubrication; (b) With SAE 5W-30 Base Oil; (c) Nanolubricant 5W-30 + (Al_2O_3); (d) Nanolubricant 5W-30 + (TiO_2); (e) Hybrid Nanolubricant 5W-30 + (Al_2O_3-TiO_2); (f) Nanolubricant 5W-30 + (Al_2O_3-PVP); (g) Nanolubricant 5W-30 + (TiO_2-PVP); (h) Hybrid Nanolubricant 5W-30 + (Al_2O_3-TiO_2-PVP)

of material and pins to the disc. This erosion is formed from the Al_2O_3 particle fraction, which produces a porosity value of 66.96%. **Figure 14d** and **Figure 15d** show the results of the wear track from the use of SAE 5W-30 and TiO_2 nanolubricant, signifying abrasion grooves accompanied by surface delamination, which is characterized by the continuous appearance of Al_2O_3 deposits on the surface. This is due to the influence of the TiO_2 particle size, which can cause surface damage because of its adhesive wear nature transformed into become abrasive wear [66]. In addition, the addition of TiO_2 nanoparticles into the base oil can reduce the level of abrasive wear, enabling the base oil to carry away the particle fragment efficiently. However, this effect is not observed on the TiO_2 lump.

In **Figure 14e** and **Figure 15e**, we can see the results of the wear track using a hybrid nanolubricant on gray cast iron FC25. The figures show the use of a hybrid nanolubricant SAE 5W-30 dan Al_2O_3, nanolubricant SAE 5W-30 and TiO_2, base oil, and without lubricant. The use of hybrid nanolubricant SAE 5W-30 can produce wider tracks but does not result in deeper scratches. Besides, the contact between hybrid nanoparticles forms tribofilms as an anti-wear protective layer that can improve the tribological nature. The porosity test results for the gray cast iron FC25 sample with the SAE 5W-30 hybrid nanolubricant were 20.718%, suggesting the superiority of hybrid nano lubricant in comparison to other types of lubricants without the addition of surfactants. The results of wear track morphology testing of gray cast iron FC25 using lubricant with the addition of PVP surfactant showed abrasive wear on the surface, as shown in **Figure 14f, Figure 14h** and **Figure 15f, Figure 15h**. Lubrication using TiO_2 produces the smoothest surface among the use of other lubricants. The rolling effect behavior of spherical nanoparticles can increase wear resistance [58]. The PVP and TiO_2 addition to the

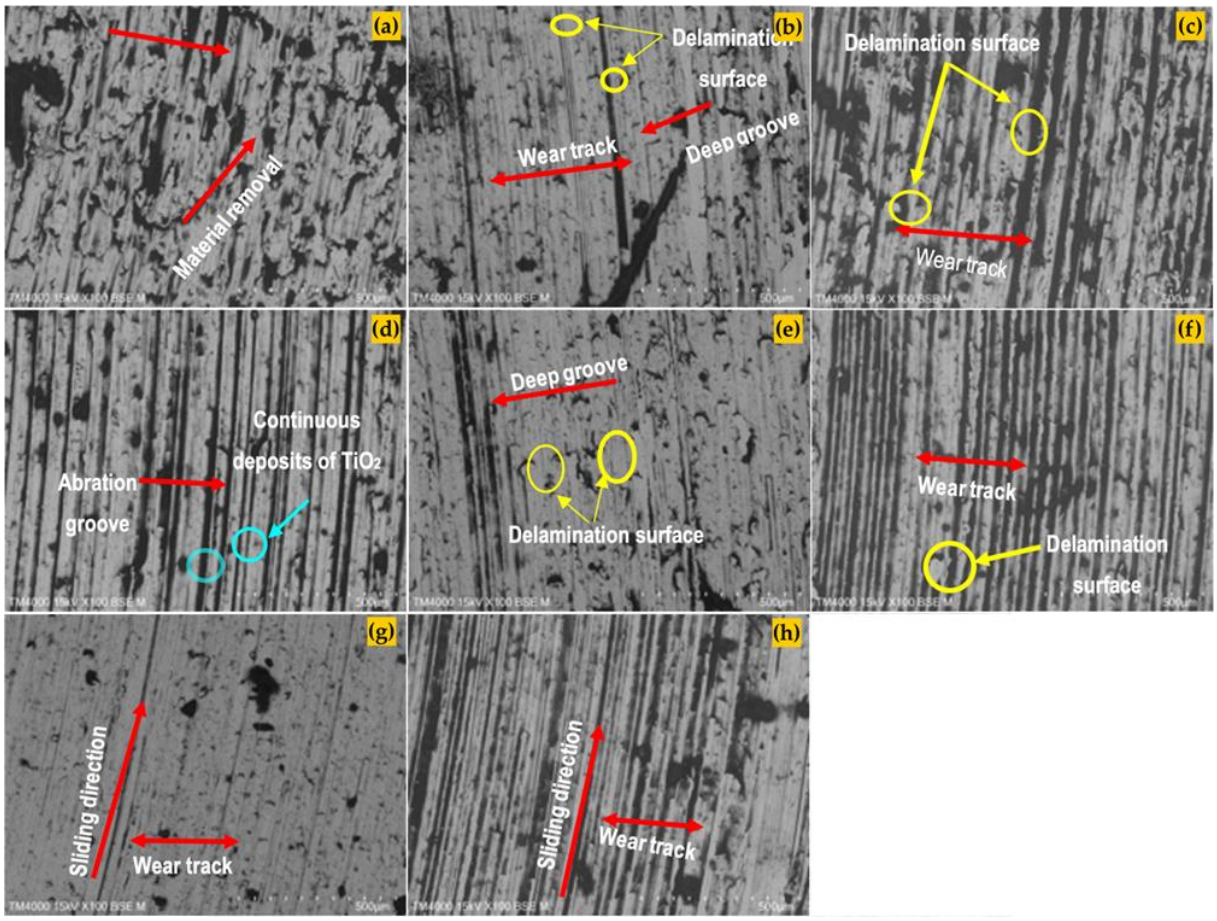

Figure 15. Morphology observation results on gray cast iron FC25 at 100x magnification (a) Without lubrication; (b) With SAE 5W-30 base oil; (c) Nanolubricant 5W-30 + (Al_2O_3); (d) Nanolubricant 5W-30 + (TiO_2); (e) Hybrid nanolubricant 5W-30 + (Al_2O_3-TiO_2); (f) Nanolubricant 5W-30 + (Al_2O_3-PVP); (g) Nanolubricant 5W-30 + (TiO_2-PVP) ;(h) Hybrid nanolubricant 5W-30 + (Al_2O_3-TiO_2-PVP)

lubricant presents low COF value than the lubricant added with PVP and Al_2O_3 or the Hybrid Al_2O_3 and TiO_2. Consequently, the gray cast iron FC25 surface coated with PVP and TiO_2 has a smoother surface as there is no significant abrasive wear [67].

4. Conclusion

In this paper, the authors have checked and applied a modified application of the multi-pass Based on the analysis results, several conclusions are discussed in the following.

The surface morphology of Aluminum Oxide nanoparticles has an irregular particle shape. The crystallite size of 20.28 nm is observed for the Aluminum Oxide nanoparticles at a peak of 2θ = 25.34º. Meanwhile, the Titanium Dioxide nanoparticles have a spherical (spherical) particle shape resembling a ball with a crystallite size of 68.06 nm, observed at a peak of 2θ = 35.04º. The functional groups of Aluminum Oxide nanoparticles are identified at the peak of 3524 – 494 $cm^{-1,}$ and the functional groups of Titanium Dioxide nanoparticles are located at the peak ranging between 3390 – 702 cm^{-1}.

The addition of nanoparticles and surfactants in SAE 5W-30 changes the thermophysical properties of the nanolubricant. The highest density (788,89 kg/mm^3) and dynamic viscosity values (0.0695 Pa.s) are obtained from the addition of PVP and TiO_2 surfactants. Meanwhile, for the nanolubricant without the addition of surfactants, the highest density (779 kg/m^3) and dynamic viscosity (0,0579 Pa.s) values are identified in the addition of hybrid Al_2O_3-TiO_2. The best stability is obtained by adding a surfactant to each nanolubricant because the addition of PVP surfactant enhances the stability of the nanolubricant.

The tribological properties of gray cast iron FC25 produce the best value of friction coefficient from the coating with SAE 5W-30 + PVP + TiO_2

(0.093), while the lowest wear mass is from the lubrication without hybrid Al_2O_3-TiO_2 surfactant (0.002 gram). The lowest surface roughness is found in a mixture of PVP and TiO_2 surfactants by 0.743 μm. The surface morphology of gray cast iron FC25 coated with SAE 5W-30 + hybrid Al_2O_3-TiO_2 and SAE 5W-30 + PVP + TiO_2 lubrication produces the smoothest surface.

Acknowledgements

Author would like to thank Universitas Negeri Malang for Hibah Penelitian KBK-Dasar 2023.

Author's Declaration

Authors' contributions and responsibilities

The authors made substantial contributions to the conception and design of the study. The authors took responsibility for data analysis, interpretation and discussion of results. The authors read and approved the final manuscript.

Funding

Hibah Penelitian KBK-Dasar 2023 Universitas Negeri Malang.

Availability of data and materials

All data are available from the authors.

Competing interests

The authors declare no competing interest.

Additional information

No additional information from the authors.

References

[1] M. Rifal, "Pengaruh Campuran Bahan Bakar Ethanol Bensin terhadap Konsumsi Bahan Bakar dan Emisi Gas Buang pada Kendaraan Bermotor 125 CC Sistem Injeksi," *Gorontalo Journal of Infrastructure and Science Engineering*, vol. 4, no. 2, pp. 50–57, 2022, doi: 10.32662/gojise.v4i2.2035.

[2] A. F. Firmansyah, A. I. Gunawan, I. A. Sulistijono, and D. Hanurawan, "Pengukuran Nilai Densitas pada Minyak Pelumas Sepeda Motor dengan Gelombang Ultrasonik," *Jurnal Rekayasa Elektrika*, vol. 18, no. 1, 2022, doi: 10.17529/jre.v18i1.24919.

[3] M. Salafudin, D. Darmanto, and T. Priangkoso, "Analisis pengaruh viskositas pelumas multi grade terhadap karakter pelumas," *Majalah Ilmiah Momentum*, vol. 16, no. 1, 2020, doi: 10.36499/jim.v16i1.3347.

[4] S. Marsela, E. W. Fridayanthie, M. Safitri, and F. Faridi, "Sistem Pendukung Keputusan Pemilihan Oli Mesin Yamaha Mio," *Jurnal Khatulistiwa Informatika*, vol. 7, no. 2, 2019, doi: 10.31294/jki.v7i2.6478.

[5] T. A. Sianturi, "Pengaruh Jenis Oli Terhadap Konsumsi Bahan Bakar pada Kenderaan Roda Dua 125 CC," *Jurnal Darma Agung*, vol. 27, no. 1, pp. 863–870, 2019, doi: 10.46930/ojsuda.v27i1.142.

[6] S. B. Mousavi and S. Z. Heris, "Experimental investigation of ZnO nanoparticles effects on thermophysical and tribological properties of diesel oil," *International Journal of Hydrogen Energy*, vol. 45, no. 43, pp. 23603–23614, 2020, doi: 10.1016/j.ijhydene.2020.05.259.

[7] H. Wu *et al.*, "Effect of water-based nanolubricant containing nano-TiO2 on friction and wear behaviour of chrome steel at ambient and elevated temperatures," *Wear*, vol. 426, pp. 792–804, 2019, doi: 10.1016/j.wear.2018.11.023.

[8] J. Lei, Z. Luo, S. Qing, X. Huang, and F. Li, "Effect of surfactants on the stability, rheological properties, and thermal conductivity of Fe3O4 nanofluids," *Powder Technology*, vol. 399, p. 117197, 2022, doi: 10.1016/j.powtec.2022.117197.

[9] A. Bajili, D. Dahlan, and A. A. Umar, "Sintesis Nanopartikel Titanium Dioksida Didoping Rhutenium," *Jurnal Ilmu Fisika*, vol. 8, no. 2, pp. 54–59, 2016, doi: 10.25077/jif.8.2.54-59.2016.

[10] W. K. Shafi and M. S. Charoo, "An overall review on the tribological, thermal and rheological properties of nanolubricants," *Tribology-Materials, Surfaces & Interfaces*, vol. 15, no. 1, pp. 20–54, 2021, doi: 10.1080/17515831.2020.1785233.

[11] W. Yu and H. Xie, "A review on nanofluids: preparation, stability mechanisms, and applications," *Journal of nanomaterials*, vol. 2012, 2012, doi: 10.1155/2012/435873.

[12] Y. Jazaa, T. Lan, S. Padalkar, and S. Sundararajan, "The effect of agglomeration reduction on the tribological behavior of WS2 and MoS2 nanoparticle additives in the boundary lubrication regime," *Lubricants*, vol. 6, no. 4, p. 106, 2018, doi: 10.3390/lubricants6040106.

[13] T. Mu, S. Leng, W. Tang, N. Shi, G. Wang, and J. Yang, "High-Performance and Low-

Cost Membranes Based on Poly (vinylpyrrolidone) and Cardo-Poly (etherketone) Blends for Vanadium Redox Flow Battery Applications," *Batteries*, vol. 8, no. 11, p. 230, 2022, doi: 10.3390/batteries8110230.

[14] S. K. Sharma, D. S. Verma, L. U. Khan, S. Kumar, and S. B. Khan, *Handbook of materials characterization*. Springer, 2018.

[15] J. Epp, "X-ray diffraction (XRD) techniques for materials characterization," in *Materials characterization using nondestructive evaluation (NDE) methods*, Elsevier, 2016, pp. 81–124.

[16] K. E. Ramohlola, E. I. Iwuoha, M. J. Hato, and K. D. Modibane, "Instrumental techniques for characterization of molybdenum disulphide nanostructures," *Journal of Analytical Methods in Chemistry*, vol. 2020, 2020, doi: 10.1155/2020/8896698.

[17] A. Kotia, P. Rajkhowa, G. S. Rao, and S. K. Ghosh, "Thermophysical and tribological properties of nanolubricants: A review," *Heat and mass transfer*, vol. 54, pp. 3493–3508, 2018, doi: 10.1007/s00231-018-2351-1.

[18] H. Budiarto and A. Adiwarna, "Pengaruh Konsentrasi Gliserin Terhadap Viskositas Dari Pembuatan Pasta Gigi Cangkang Kerang Darah," *Jurnal Konversi*, vol. 2, no. 1, 2013, doi: 10.24853/konversi.2.1.%25p.

[19] J. Zhao, Y. Huang, Y. He, and Y. Shi, "Nanolubricant additives: A review," *Friction*, vol. 9, pp. 891–917, 2021, doi: 10.1007/s40544-020-0450-8.

[20] P. P. Patil, Y. Gori, A. Kumar, and M. R. Tyagi, "Experimental analysis of tribological properties of polyisobutylene thickened oil in lubricated contacts," *Tribology International*, vol. 159, p. 106983, 2021, doi: 10.1016/j.triboint.2021.106983.

[21] J. Salguero, J. M. Vazquez-Martinez, I. Del Sol, and M. Batista, "Application of pin-on-disc techniques for the study of tribological interferences in the dry machining of A92024-T3 (Al–Cu) alloys," *Materials*, vol. 11, no. 7, p. 1236, 2018, doi: 10.3390/ma11071236.

[22] D. Gasni, K. M. A. Razak, A. Ridwan, and M. Arif, "Pengaruh Penambahan Minyak Kelapa dan Sawit Terhadap Sifat Fisik dan Tribologi Pelumas SAE 40," *Jurnal METTEK Volume*, vol. 5, no. 1, pp. 1–9, 2019, doi: 10.24843/METTEK.2019.v05.i01.p01.

[23] D. Z. Segu and P. Hwang, "Friction control by multi-shape textured surface under pin-on-disc test," *Tribology International*, vol. 91, pp. 111–117, 2015, doi: 10.1016/j.triboint.2015.06.028.

[24] N. E. Wahyuningtiyas and H. Suryanto, "Analysis of biodegradation of bioplastics made of cassava starch," *Journal of Mechanical Engineering Science and Technology (JMEST)*, vol. 1, no. 1, pp. 24–31, 2017, doi: 10.17977/um016v1i12017p024.

[25] P. Puspitasari, M. A. Iftiharsa, H. F. N. Zhorifah, and R. W. Gayatri, "Analysis of physical properties and compressibility of avian eggshell nanopowders in solid state reaction," *EUREKA: Physics and Engineering*, vol. 5, pp. 110–120, 2021, doi: 10.21303/2461-4262.2021.001670.

[26] N. S. Yüzbasi *et al.*, "Removal of MS2 and fr bacteriophages using MgAl2O4-modified, Al2O3-stabilized porous ceramic granules for drinking water treatment," *Membranes*, vol. 12, no. 5, p. 471, 2022, doi: 10.3390/membranes12050471.

[27] N. Nasution and A. Fitri, "Synthesis of Rutile TIO2 Nanoparticles by Co-precipitation Method," *Fisitek: Jurnal Ilmu Fisika dan Teknologi*, vol. 2, no. 2, 2018, doi: 10.30821/fisitek.v2i2.1808.

[28] P. Puspitasari, M. Chairil, S. Sukarni, and N. S. W. Supriyanto, "Physical properties and compressibility of quail eggshell nanopowder with heat treatment temperature variations," *Materials Research Express*, vol. 8, no. 5, p. 55008, 2021, doi: 10.1088/2053-1591/ac0266.

[29] K. A. Bokhary, F. Maqsood, M. Amina, A. Aldarwesh, H. K. Mofty, and H. M. Al-Yousef, "Grapefruit extract-mediated fabrication of photosensitive aluminum oxide nanoparticle and their antioxidant and anti-inflammatory potential," *Nanomaterials*, vol. 12, no. 11, p. 1885, 2022, doi: 10.3390/nano12111885.

[30] P. Puspitasari and D. D. Pramono, "Phase Identification, Morphology, and Compressibility of Scallop Shell Powder (Amusium Pleuronectes) for Bone Implant Materials," in *Nanotechnologies in Green Chemistry and Environmental Sustainability*, CRC Press, 2022, pp. 5–25.

[31] D. D. Pramono, P. Puspitasari, A. A. Permanasari, S. Sukarni, and A. Wahyudiono, "Effect of sintering time on porosity and compressibility of calcium carbonate from Amusium pleuronectes (scallop shell)," in *AIP Conference Proceedings*, 2023, vol. 2687, no. 1, doi: 10.1063/5.0120990.

[32] G. A. Nowsherwan *et al.*, "Preparation and Numerical Optimization of TiO2: CdS Thin Films in Double Perovskite Solar Cell," *Energies*, vol. 16, no. 2, p. 900, 2023, doi: 10.3390/en16020900.

[33] J. Maulana, H. Suryanto, and A. Aminnudin, "Effect of graphene addition on bacterial cellulose-based nanocomposite," *Journal of Mechanical Engineering Science and Technology (JMEST)*, vol. 6, no. 2, pp. 107–116, 2022, doi: 10.17977/um016v6i22022p107.

[34] E. A. Arafat *et al.*, "Entomotherapeutic Role of Periplaneta americana Extract in Alleviating Aluminum Oxide Nanoparticles-Induced Testicular Oxidative Impairment in Migratory Locusts (Locusta migratoria) as an Ecotoxicological Model," *Antioxidants*, vol. 12, no. 3, p. 653, 2023, doi: 10.3390/antiox12030653.

[35] X. Liang *et al.*, "Preparation of Anticorrosive Epoxy Nanocomposite Coating Modified by Polyethyleneimine Nano-Alumina," *Coatings*, vol. 13, no. 3, p. 561, 2023, doi: 10.3390/coatings13030561.

[36] D. Domyati, "Chemical and thermal study of metal chalcogenides (zinc sulfide), aluminum oxide, and graphene oxide based nanocomposites for wastewater treatment," *Ceramics International*, vol. 49, no. 1, pp. 1464–1472, 2023, doi: 10.1016/j.ceramint.2022.09.190.

[37] M. Bartoszewska, E. Adamska, A. Kowalska, and B. Grobelna, "Novelty Cosmetic Filters Based on Nanomaterials Composed of Titanium Dioxide Nanoparticles," *Molecules*, vol. 28, no. 2, p. 645, 2023, doi: 10.3390/molecules28020645.

[38] M. N. Nduni, A. M. Osano, and B. Chaka, "Synthesis and characterization of aluminium oxide nanoparticles from waste aluminium foil and potential application in aluminium-ion cell," *Cleaner Engineering and Technology*, vol. 3, p. 100108, 2021, doi: 10.1016/j.clet.2021.100108.

[39] S. Q. Wang, W. B. Liu, P. Fu, and W. L. Cheng, "Enhanced photoactivity of N-doped TiO 2 for Cr (VI) removal: Influencing factors and mechanism," *Korean Journal of Chemical Engineering*, vol. 34, pp. 1584–1590, 2017, doi: 10.1007/s11814-017-0003-7.

[40] A. Piątkowska, M. Janus, K. Szymański, and S. Mozia, "C-, N-and S-doped TiO2 photocatalysts: a review," *Catalysts*, vol. 11, no. 1, p. 144, 2021, doi: 10.3390/catal11010144.

[41] D. Heltina, U. Avisa, and M. I. Fermi, "The role of surfactant to enhance photocatalyst performance on phenol degradation in TiO2-CNT composite-modified CNT (Cetyltrimethylammonium bromide)," in *IOP Conference Series: Materials Science and Engineering*, 2021, vol. 1041, no. 1, p. 12048, doi: 10.1088/1757-899X/1041/1/012048.

[42] C. S. Wiguna, H. Suryanto, A. Aminnudin, J. S. Binoj, and A. Ali, "Effect of Grafting Nano-TiO2 on Sansevieria Cylindrica Fiber Properties," *Journal of Mechanical Engineering Science and Technology (JMEST)*, vol. 7, no. 1, pp. 10–19, 2023, doi: 10.17977/um016v7i12023010.

[43] M. R. Purwanto, P. Puspitasari, A. A. Permanasari, and M. Abdullah, "Investigation of Thermophysical and Rheological Properties of Scallop Shell Powder/SAE 5w-30 Nanolubricant," *Transmisi*, vol. 19, no. 1, pp. 30–36, 2023, doi: 10.26905/jtmt.v19i1.9638.

[44] M. F. Nabil, W. H. Azmi, K. A. Hamid, N. N. M. Zawawi, G. Priyandoko, and R. Mamat, "Thermo-physical properties of hybrid nanofluids and hybrid nanolubricants: a comprehensive review on performance," *International Communications in Heat and Mass Transfer*, vol. 83, pp. 30–39, 2017, doi: 10.1016/j.icheatmasstransfer.2017.03.008.

[45] C. Birleanu, M. Pustan, M. Cioaza, A. Molea, F. Popa, and G. Contiu, "Effect of TiO2 nanoparticles on the tribological properties of lubricating oil: an experimental investigation," *Scientific Reports*, vol. 12, no. 1, p. 5201, 2022, doi: 10.1038/s41598-022-09245-2.

[46] M. K. A. Ali and H. Xianjun, "Improving the heat transfer capability and thermal stability of vehicle engine oils using Al2O3/TiO2 nanomaterials," *Powder Technology*, vol. 363,

pp. 48–58, 2020, doi: 10.1016/j.powtec.2019.12.051.

[47] P. Puspitasari, S. B. Khoyroh, A. A. Permanasari, M. M. A. Pratama, and S. A. A. Karim, "Analysis of the Thermophysical Properties of SAE 5W-30 Lubricants with the Addition of Al2O3, TiO2, and Hybrid Al2O3-TiO2 Nanomaterials on the Performance of Motorcycles," in *Nanotechnologies in Green Chemistry and Environmental Sustainability*, 1st ed., CRC Press, 2022.

[48] R. K. Asmoro, P. Puspitasari, A. A. Permanasari, and M. Abdullah, "Identification of Thermophysical and Rheological Properties of SAE 5w-30 with Addition of Hexagonal Boron Nitride," *Transmisi*, vol. 19, no. 1, pp. 41–48, 2023, doi: 10.26905/jtmt.v19i1.9639.

[49] M. Bahrami, M. Akbari, A. Karimipour, and M. Afrand, "An experimental study on rheological behavior of hybrid nanofluids made of iron and copper oxide in a binary mixture of water and ethylene glycol: non-Newtonian behavior," *Experimental Thermal and Fluid Science*, vol. 79, pp. 231–237, 2016, doi: 10.1016/j.expthermflusci.2016.07.015.

[50] L. S. Sundar, G. O. Irurueta, E. V. Ramana, M. K. Singh, and A. C. M. Sousa, "Thermal conductivity and viscosity of hybrid nanfluids prepared with magnetic nanodiamond-cobalt oxide (ND-Co3O4) nanocomposite," *Case studies in thermal engineering*, vol. 7, pp. 66–77, 2016, doi: 10.1016/j.csite.2016.03.001.

[51] J. Sarkar, P. Ghosh, and A. Adil, "A review on hybrid nanofluids: recent research, development and applications," *Renewable and Sustainable Energy Reviews*, vol. 43, pp. 164–177, 2015, doi: 10.1016/j.rser.2014.11.023.

[52] T. Luo, X. Wei, H. Zhao, G. Cai, and X. Zheng, "Tribology properties of Al2O3/TiO2 nanocomposites as lubricant additives," *Ceramics International*, vol. 40, no. 7, pp. 10103–10109, 2014, doi: 10.1016/j.ceramint.2014.03.181.

[53] Y. Sun, C. Jiang, Q. Zhao, X. Wang, and W. Lou, "Tribo-Dependent Photoluminescent Behavior of Oleylamine-Modified AgInS2 and AgInS2-ZnS Nanoparticles as Lubricant Additives," *Lubricants*, vol. 11, no. 7, p. 280, 2023, doi: 10.3390/lubricants11070280.

[54] M. Molaei, A. Fattah-Alhosseini, M. Nouri, and M. Kaseem, "Role of TiO2 Nanoparticles in Wet Friction and Wear Properties of PEO Coatings Developed on Pure Titanium," *Metals*, vol. 13, no. 4, p. 821, 2023, doi: 10.3390/met13040821.

[55] Y. Gao, M. H. Vini, S. Daneshmand, A. A. Alameri, O. Benjeddou, and R. H. C. Alfilh, "Effect of Processing Parameters on Wear Properties of Hybrid AA1050/Al2O3/TiO2 Composites," *Crystals*, vol. 13, no. 2, p. 335, 2023, doi: 10.3390/cryst13020335.

[56] P. Puspitasari, D. D. Pramono, C. S. Putra, A. A. Permanasari, A. M. H. S. Lubis, and M. I. H. C. Abdullah, "Optimization of Performance Carbon-Based Nanolubricant on Ti6Al4V Pin on Disc Testing Using Taguchi Method," in *2023 8th International Conference on Electrical, Electronics and Information Engineering (ICEEIE)*, 2023, pp. 1–5.

[57] L. Peña-Parás *et al.*, "Effects of substrate surface roughness and nano/micro particle additive size on friction and wear in lubricated sliding," *Tribology International*, vol. 119, pp. 88–98, 2018, doi: 10.1016/j.triboint.2017.09.009.

[58] L. Peña-Parás, J. Taha-Tijerina, L. Garza, D. Maldonado-Cortés, R. Michalczewski, and C. Lapray, "Effect of CuO and Al2O3 nanoparticle additives on the tribological behavior of fully formulated oils," *Wear*, vol. 332, pp. 1256–1261, 2015, doi: 10.1016/j.wear.2015.02.038.

[59] M. K. A. Ali, H. Xianjun, L. Mai, C. Qingping, R. F. Turkson, and C. Bicheng, "Improving the tribological characteristics of piston ring assembly in automotive engines using Al2O3 and TiO2 nanomaterials as nano-lubricant additives," *Tribology International*, vol. 103, pp. 540–554, 2016, doi: 10.1016/j.triboint.2016.08.011.

[60] R. Molaei, M. R. Zali, M. H. Mobaraki, and J. Y. Farsi, "The impact of entrepreneurial ideas and cognitive style on students entrepreneurial intention," *Journal of Entrepreneurship in Emerging Economies*, vol. 6, no. 2, pp. 140–162, 2014, doi: 10.1108/JEEE-09-2013-0021.

[61] E. M. Bortoleto *et al.*, "Experimental and numerical analysis of dry contact in the pin

on disc test," *Wear*, vol. 301, no. 1–2, pp. 19–26, 2013, doi: 10.1016/j.wear.2012.12.005.

[62] M. Garcia Lleo *et al.*, "Enhanced Tribology of Top-Down Graphene as Efficient Additive in Commercial Engine Oils," *Available at SSRN 4392553*.

[63] M. Abdullah, M. F. B. Abdollah, H. Amiruddin, N. Tamaldin, and N. R. M. Nuri, "Effect of hBN/Al2O3 nanoparticle additives on the tribological performance of engine oil," *Jurnal Teknologi*, vol. 66, no. 3, pp. 1–6, 2014, doi: 10.11113/jt.v66.2685.

[64] F. Ilie and C. Covaliu, "Tribological properties of the lubricant containing titanium dioxide nanoparticles as an additive," *Lubricants*, vol. 4, no. 2, p. 12, 2016, doi: 10.3390/lubricants4020012.

[65] M. K. Ahmed Ali, H. Xianjun, F. A. Essa, M. A. A. Abdelkareem, A. Elagouz, and S. W. Sharshir, "Friction and wear reduction mechanisms of the reciprocating contact interfaces using nanolubricant under different loads and speeds," *Journal of Tribology*, vol. 140, no. 5, p. 51606, 2018, doi: 10.1115/1.4039720.

[66] P. Puspitasari, A. A. Permanasari, M. I. H. C. Abdullah, D. D. Pramono, and O. J. Silaban, "Tribology Characteristic of Ball Bearing SKF RB-12.7/G20W using SAE 5W-30 Lubricant with Carbon-Based Nanomaterial Addition," *Tribology in Industry*, vol. 45, no. 3, 2023, doi: 10.24874/ti.1538.09.23.11.

[67] S. Azam and S.-S. Park, "Sonochemical Synthesis of CuO Nanoplatelets and Their Tribological Properties as an Additive in Synthetic Oil Using Reciprocating Tribometer," *Lubricants*, vol. 11, no. 4, p. 185, 2023, doi: 10.3390/lubricants11040185.